Journal of Applied Sciences

ISSN 1812-5654

science alert

ANSInet
an open access publisher
http://ansinet.com

Journal of Applied Sciences 13 (16): 3128-3136, 2013
ISSN 1812-5654 / DOI: 10.3923/jas.2013.3128.3136

Modeling and Feather Extraction of Rotating Rectifier Faults of Aircraft Integrated Drive Generator

[1,2]Xudong Shi, [3]Pengju Li, [3]Jijun Zhu, [4]Hongwen Ma and [5]Jianqun Han
[1]Tianjin Key Laboratory for Civil Aircraft Airworthiness and Maintenance of Civil Aviation, University of China, Tianjin, 300300, China
[2]Ground Support Equipments Research Base of Civil Aviation University of China, Tianjin, 300300, China
[3]Aeronautical Automation College, Civil Aviation University of China, Tianjin, 300300, China
[4]Mechanicaland Electrical Engineering College of Harbin Engineering University, Heilongjiang, 150001, China
[5]Engineering College of Bohai University, Jinzhou, Liaoning C121013, China

Abstract: As the power system capacity of airliner is increasing, brushless excitation has been applied to the aircraft generator. The voltage and current of rotating rectifier cannot be measured directly because of the elimination of carbon brushes and slip rings in excitation system, so the faults cannot be detected. There is an effective way to detect faults according to the features reflected in the stator field winding. Firstly, the fault mechanism of rotating rectifier is studied based on harmonic analysis. Next, the common faults of rectifier diode are classified and the aircraft generator simulation model is established to observe the generator output and stator field current. Finally, the feather of fault signal is extracted based on harmonic analysis, laying the foundation for further fault diagnosis of rotating rectifier in aircraft IDG.

Key words: Aircraft IDG, rotating rectifier, stator field current, harmonic analysis

INTRODUCTION

Aircraft IDG (Integrated Drive Generator) has been widely used in airborne power of modern transport aircraft with its small bulk and high reliability. Three-level brushless AC synchronous generator is employed in IDG, where permanent magnet generator is used as sub-exciter and the exciter and generator are rotating-armature and rotating-magnetic synchronous generator, respectively. They are installed on the same shaft driven by the engine and the CSD (Constant Speed Drive) unit provides the constant speed. The generator outputs three-phase AC of 115 V 400 Hz^{-1}.

The magnetic field of generator is provided by exciter. The three-phase AC output by exciter is rectified to DC by the rectifier bridge on rotor armature as field current of generator. The rectifier bridge is called rotating rectifier since it rotates along with the spindle. The rotating rectifier composed by power diodes and rotating disk is the most important part of the brushless excitation system, while it is prone to failure due to the low pressure and high temperature and other adverse factors that exist in aircraft. Fault detection and diagnosis for the rotating rectifier is particularly important to ensure normal operation of the excitation system, on which domestic and foreign scholars have done a lot of research. Wang *et al.* (2006) extracted the induced EMF (Electromotive Force) of exciter stator coil, analyzing and determining potential failure by immune algorithm. Zhang and Xia (2009) aimed at excitation circuit of exciter, regarding field current as non-stationary signals and analyzing it by fractal theory, while the algorithm is complex and the sensitivity is poor. Lots of documents show that researches on rotating rectifier fault diagnosis method mainly focus on analysis of fault signals. Many of these analysis are qualitative description, lacking systematic classification of rotating rectifier fault. A simulation model of three-level generator system is established in this paper, focusing on the analysis of the excitation part and classifying faults according to the working principle of rectifier circuit. Then the stator field current under fault is attained for harmonic analysis. Finally the feather of fault signal is extracted, thereby providing a basis for rotating rectifier fault diagnosis.

FAULT ANALYSIS FOR ROTATING RECTIFIER

Theoretical analysis of rotating rectifier operating normally: The AC exciter in brushless excitation system is loaded with rotating rectifier, so the output current is

Corresponding Author: Pengju Li, Aeronautical Automation College, Civil Aviation University of China, Tianjin, 300300, China
Tel: +86 13920317307

distorted and is not a sine wave instead. The load of rectifier circuit - the generator excitation winding, can be seen as an inductive load. Ideally, the output of AC exciter is close to a rectangular wave. The width of each phase armature winding is $2\pi/3$ and the height is I_d. The structure of excitation system is shown in Fig. 1. E_e is the electric potential of the exciter stator windings. I_e is the stator winding current. E_a, E_b and E_c is the three-phase EMF. I_d is the load current, that is the generator field current I_f.

The exciter of aircraft IDG is the rotating armature generator, so the faults of rotating rectifier cannot be diagnosed by measuring the rotor armature current. When a fault occurs, the exciter rotor armature current I_{fa} will produce an armature-reaction MMF (Magnetomotive Force) that is different from the normal operation. Thereby the harmonic characteristics of the exciter stator field current I_{ff} will be affected by the abnormal MMF and thus a certain distortion will be produced (Batzel *et al.*, 2003). The nature of armature-reaction MMF when non-sinusoidal current flowing through the armature winding is analyzed firstly.

In the three-phase AC exciter, the difference of electrical angle between winding current per phase is $2\pi/3$ and the winding current per phase i_k (k = 1, 2, 3) is

$$i_k = \sqrt{2} I_\mu \cos\mu[\omega t - (k-1)\frac{2}{3}\pi] \quad (1)$$

The MMF of phase k winding is

$$f_k = F_{\mu-\nu}\frac{i_k}{\sqrt{2}I_\mu}\cos\nu[\alpha - (k-1)\frac{2}{3}\pi] \quad (2)$$

I_μ is the RMS of the μth harmonic of each phase winding current and í is the harmonic order of MMF and $F_{\mu-í}$ is the MMF magnitude for each phase winding. As seen by the electromechanics theory (Li and Zhu, 2007):

$$F_{\mu-\nu} = \frac{2\sqrt{2}}{\pi}\frac{Nk_{dq\nu}}{\nu p} = \frac{2\sqrt{2}}{\pi}\frac{NI_\mu}{\nu p}\frac{\sin q\frac{\nu\theta}{2}}{q\sin\frac{\nu\theta}{2}}\sin\nu\frac{y\pi}{2} \quad (3)$$

N is the number of series turns of the phase windings and P is the number of pole pairs and q is the number of slots of each phase of each pole and θ is the slot-pitch angle and y is the short-pitch ratio of the winding.

The synthetic MMF of the three-phase windings is attained by Eq. 1 and 2.

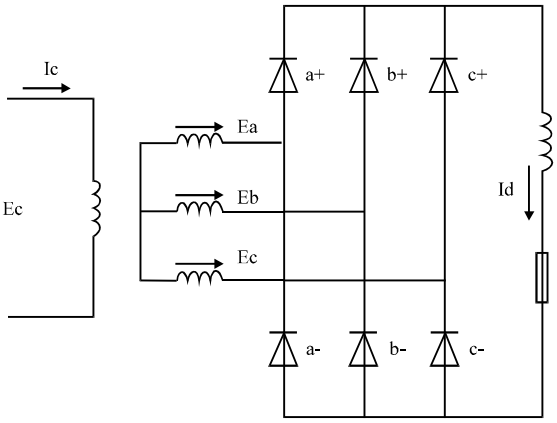

Fig. 1: Structure diagram of brushless excitation system

$$f_{\nu\Sigma} = \sum_{k=1}^{3} f_k = \sum_{k=1}^{3} F_{\mu-\nu}\cos\nu[\alpha - (k-1)\frac{2}{3}\pi]\cdot\cos\mu[\omega t - (k-1)\frac{2}{3}\pi] \quad (4)$$

In the above equation, $f_{\nu\Sigma}$ is the νth synthetic MMF generated by the μth harmonic of the stator current on a 3-phase synchronous exciter. The MMF generated by each phase winding is a pulsating MMF, that can be decomposed into the synthesis of two MMF rotating reversely.

$$f_{\nu\Sigma} = f^-_{\nu\Sigma} + f^+_{\nu\Sigma} = \frac{1}{2}F_{\mu-\nu}\sum_{k=1}^{3}\cos[(\nu\alpha + \mu\omega t) - (\mu+\nu)(k-1)\frac{2}{3}\pi] + \frac{1}{2}F_{\mu-\nu}\sum_{k=1}^{3}\cos[(\nu\alpha - \mu\omega t) + (\mu-\nu)(k-1)\frac{2}{3}\pi] \quad (5)$$

After further theoretical derivation of the above formula, it is shown that there are only the (3k-μ)th reverse rotating component and the (3k+μ)th forward rotating component existing in the armature reaction MMF. When μ = 1, the (3k+1)th harmonics MMF generated by the armature fundamental current rotates in the opposite direction with the rotor and the (3k-1)th harmonics MMF rotates in the same direction with the rotor and then both of them will generate the 3kth harmonics EMF in the stator windings. Similarly, when μ=n, the (3k±n)th harmonic MMF generated by the armature harmonic current will generate the 3kth harmonics EMF in the stator windings. Therefore, the induced EMF in the exciter stator winding mainly contains the 3kth harmonics when the three-phase exciter operates normally. It is shown by further analysis that the EMF induced by even harmonic components is 0 in the excitation winding, therefore the EMF induced by the 2nd

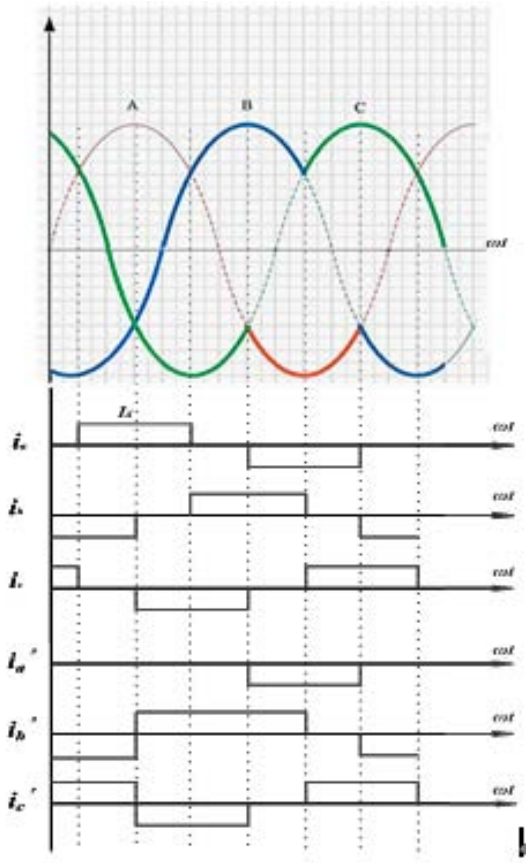

Fig. 2: Schematic diagram of circuit conduction of rectifiers under a+ diode open-circuit fault

and 4th harmonic MMF is 0 in the three-phase exciter. In conclusion, the stator field current in the three-phase exciter mainly contains the 6th harmonics except the DC component (Wakileh, 2011).

Harmonic analysis for the exciter stator current under rotating rectifier fault: To take a+diode open-circuit fault as an example, the circuit conduction waveform of rectifiers is shown in Fig. 2. The conduction order of diodes will become: c+/b- > b+/c- > b+/a- > c+/a-. In the 1/3 cycle of $\pi/6$ to $5\pi/6$, the conduction is abnormal and the waveform of I_{fa} is distorted, thus the I_{ff} is distorted according to the armature reaction characteristics.

As shown in Fig. 2, $i_a.i_b.i_c$ are the armature current in normal state and $i_a'.i_b'.i_c'$ are the armature current under a+diode open-circuit fault. It is clear that the ABC three-phase armature current will all distort due to the fault (Na, 2011). Therefore the ABC three-phase armature current under the fault can be seen as the superposition of the armature current in normal state and $\Delta i_a.\Delta i_b.\Delta i_c$, that is:

$$\begin{cases} i_a' = i_a + \Delta i_a \\ i_b' = i_b + \Delta i_b \\ i_c' = i_c + \Delta i_c \end{cases} \tag{6}$$

Where:

$$\Delta i_a = \begin{cases} -I_d & (\frac{\pi}{6}, \frac{5\pi}{6}) \\ 0 & (0, \frac{\pi}{6})(\frac{5\pi}{6}, 2\pi) \end{cases} \tag{7}$$

$$\Delta i_b = \begin{cases} I_d & (\frac{\pi}{2}, \frac{5\pi}{6}) \\ 0 & (0, \frac{\pi}{2})(\frac{5\pi}{6}, 2\pi) \end{cases} \tag{8}$$

$$\Delta i_c = \begin{cases} I_d & (\frac{\pi}{6}, \frac{\pi}{2}) \\ 0 & (0, \frac{\pi}{6})(\frac{\pi}{2}, 2\pi) \end{cases} \tag{9}$$

Implement Fourier analysis on Δi_a:

$$\begin{aligned} \Delta i_a &= a_0 + \sum_{n=1}^{\infty}(a_n \cos n\omega t + b_n \sin n\omega t) \\ &= -\frac{1}{3} I_d + \sum_{n=1}^{\infty} \sqrt{a_n^2 + b_n^2} \sin(n\omega t + \arctan \frac{a_n}{b_n}) \end{aligned} \tag{10}$$

Take the first five terms for calculations:

$$\begin{aligned} \Delta i_a = -\frac{1}{3} I_d + 0.552 I_d \sin \omega t + 0.276 I_d \sin(2\omega t + 90°) \\ + 0.138 \sin(4\omega t + 90°) \end{aligned} \tag{11}$$

Similarly:

$$\begin{aligned} \Delta i_b = \frac{1}{6} I_d + 0.319 I_d \sin(\omega t - 30°) + 0.276 I_d \sin(2\omega t + 30°) \\ 0.212 I_d \sin(3\omega t + 90°) + 0.138 I_d \sin(4\omega t - 30°) \end{aligned} \tag{12}$$

$$\begin{aligned} \Delta i_c = \frac{1}{6} I_d + 0.319 I_d \sin(\omega t + 30°) + 0.276 I_d \sin(2\omega t - 30°) \\ 0.212 I_d \sin(3\omega t - 90°) + 0.138 I_d \sin(4\omega t + 30°) \end{aligned} \tag{13}$$

It is clear that there are DC component and harmonic components coexisting in $\Delta i_a.\Delta i_b.\Delta i_c$ (Boggess and Narcowich, 2002). The methods of analyzing the harmonic characteristics of stator current I_{ff} under one diode open-circuit fault is consistent with that in normal state.

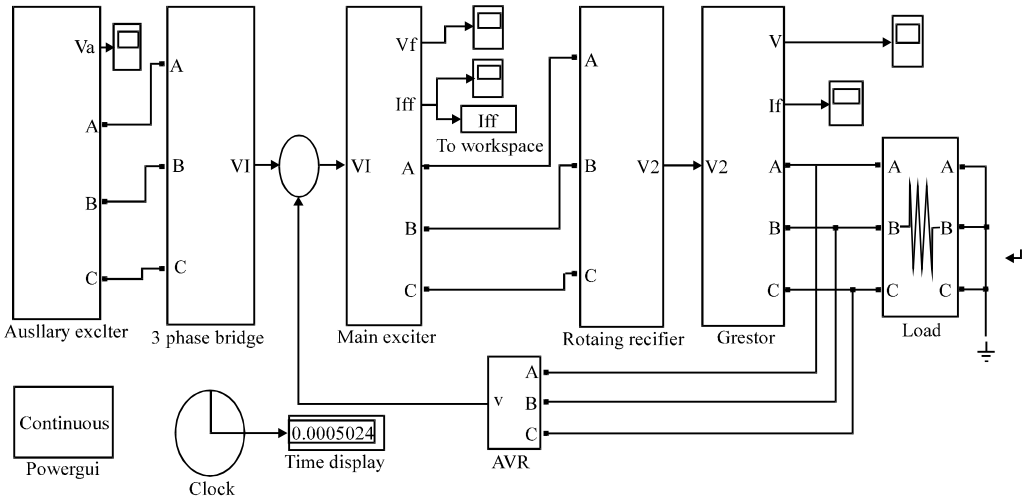

Fig. 3: Simulation model of three-level generator system

Table 1: Fault pattern classification of rotating rectifier

Fault type	Typical example	Other similar models
One diode open-circuit	+a open-circuit	+b, c+, a-, b-, c-
Two diodes open-circuit	a+a- open-circuit	b+b-, c+c-
Two diodes open-circuit in one phase	a+a- open-circuit	a+c+, a-b-
Two diodes open-circuit in the same bridge arm	a+b+ open-circuit	a+c-, a-b+
One diode short-circuit	+a short-circuit	-b, c+, a-, b-, c-
Two diodes short-circuit in different phases and bridge arms	a+b- short-circuit	a+c-, a-b+
Two diodes short-cirucit in different phase and bridge arms	a+b- short-circuit	a+c-, a-b+

Finally it is clear after analysis that the exciter stator current under one-diode open-circuit fault contains fundamental and low-frequency harmonic such 2nd, 3rd and 4th harmonic, in addition to containing a DC component and 6th harmonic.

FAULT MODELING AND SIMULATION OF ROTATING RECTIFIER

Since the six diodes are turned on sequentially, rectifier faults can be classified into several categories based on permutations. When short-circuit fault occurs, the generator field current will decrease substantially and the aircraft power will supply insufficient electricity. What's more, a large short-circuit current will flow through the non-shorted diodes that are prone to burn out if not treated timely, resulting in the disfunction of generator. Therefore, rapid diagnostic for shorted diodes is greatly significant. When open-circuit fault occurs, the rectifier coefficient of diode rectifier will decrease. In order to keep the generator output voltage in constant, the generator field current will increase under the action of the AVR (Automatic Voltage Regulator) and the generator can still run sickly.

Fault pattern classification of rotating rectifier: Current waveform of other types of fault can be analyzed by the same method as one diode open-circuit fault mentioned above. Given the big probability of faults occurring in one or two diodes, generator rotating rectifier faults can be divided into seven categories according to the I_{ff} distortion rules measured in simulation experiments, as is shown in Table 1.

Modeling and simulation of three-level generators: Three-level synchronous AC generator is a separate-excitation generator with features of reliable excitation initiating. It consists of three generators. The 1st level is a permanent magnet synchronous generator and the 2nd and 3th level are electrically excited synchronous generators. The Matlab/Simulink simulation model is constructed according to the mathematical equations of synchronous generator, as shown in Fig. 3 (Mouni *et al*., 2008; Hydro-Qubec, 2008).

The main-exciter stator field current I_{ff}, which is extracted to Workplace in Matlab for algorithm analysis, is the primary basis for analyzing rectifier faults. AVR severs as the three feedback loops of three-level generator system to ensure that the generator can still run sickly.

In the rotating rectifier module, ideal switches are respectively in series/parallel with the six diodes. Diode short-circuit or open-circuit fault simulation can be achieved at a certain moment by controlling the switches on-off by the timers, as shown in Fig. 4.

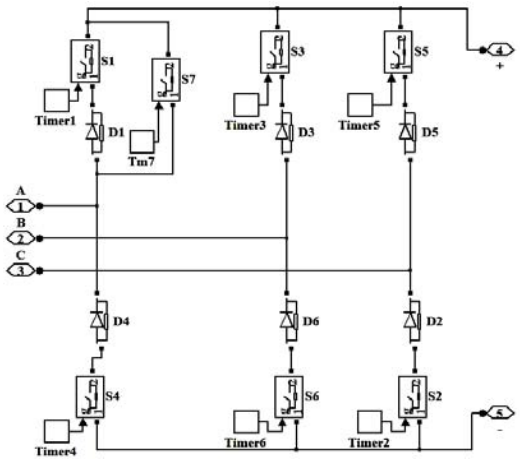

Fig. 4: Fault simulation model of rotating rectifier

The simulation time is set as 0.1 sec. The switch S1 is switched off at the time of 0.05 sec to simulate the one diode open-circuit fault (take a+ open-circuit as example). In Fig. 5, the upper figure is the simulation result of the exciter field current I_{ff} and the following figures are partial magnification of I_{ff} in normal state and under the fault. As mentioned above, the ripple wave of exciter stator current is mainly 6th harmonics.

The three-phase output of the generator is shown in Fig. 6a and the RMS voltage is shown in b. The prefault output voltage stabilizes at 115 V 400 Hz^{-1}.While the voltage decreases under fault and tends towards stability under the control of AVR. The result has a certain steady-state error due to the nature of the control system itself, while the generator can still run sickly.

The following figures show the simulation waveforms of the exciter stator current I_{ff} when the other six kinds of faults occur in rotating rectifier. The starting time of each fault simulation is set to 0.05 sec. The upper figure shows the fault waveform comparison of I_{ff} before and after fault and the following figure shows the partial magnification of I_{ff} under fault. It is clear that the harmonic characteristics or RMS of I_{ff} under each fault are different.

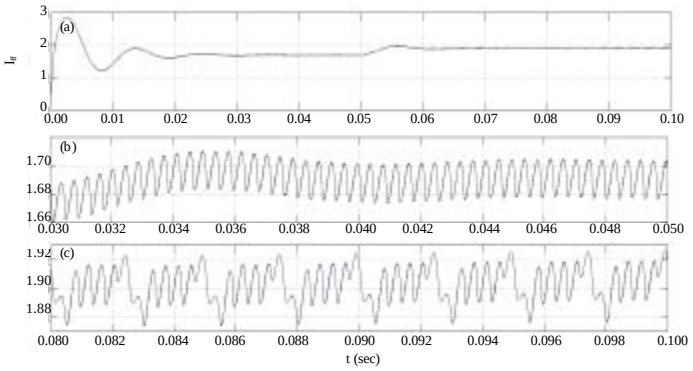

Fig. 5(a-c): Exciter stator current I_{ff} under one diode open-circuit fault, (a) Simulation results of the excites field current Iff, (b) Partial magnification of Iff in normal state and (c) Partial magnification of Iff in normal state under fault

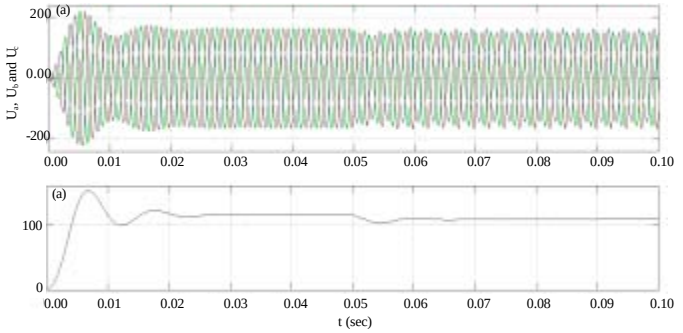

Fig. 6: The three-phase output of the generator-UaandUbandUc

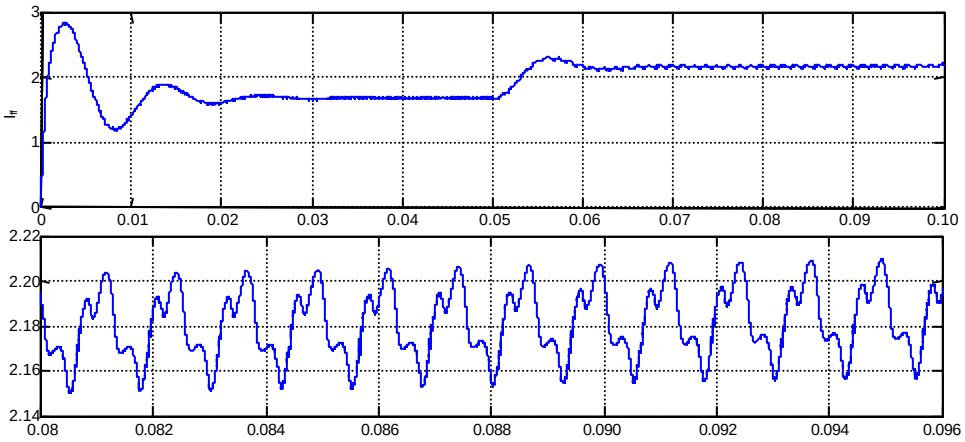

Fig. 7: Exciter stator current I_{ff} under two diodes open-circuit in one-phase fault

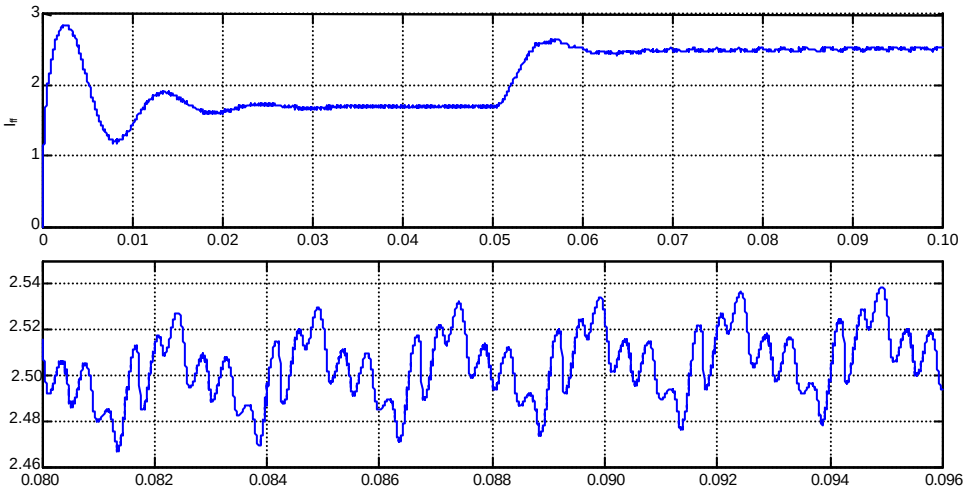

Fig. 8: Exciter stator current I_{ff} under two diodes open-circuit in the same bridge arm fault

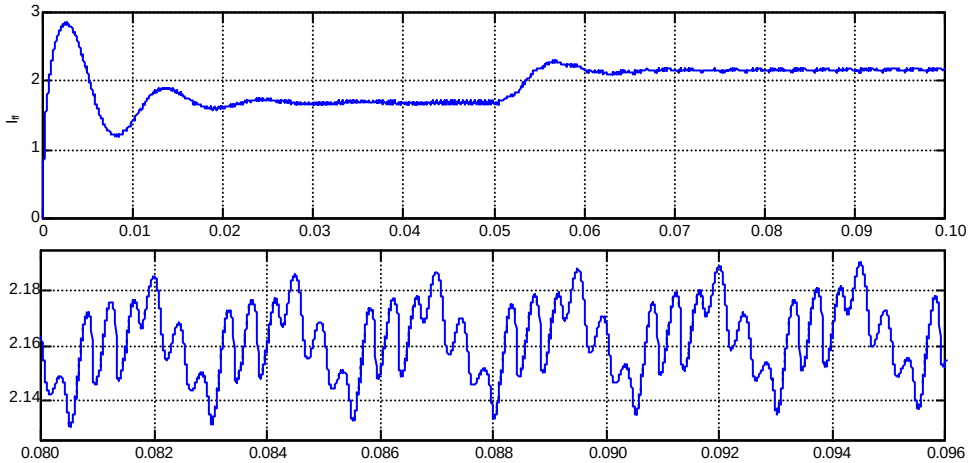

Fig. 9: Exciter stator current I_{ff} under two diodes open-circuit in different phases and bridge- arms fault

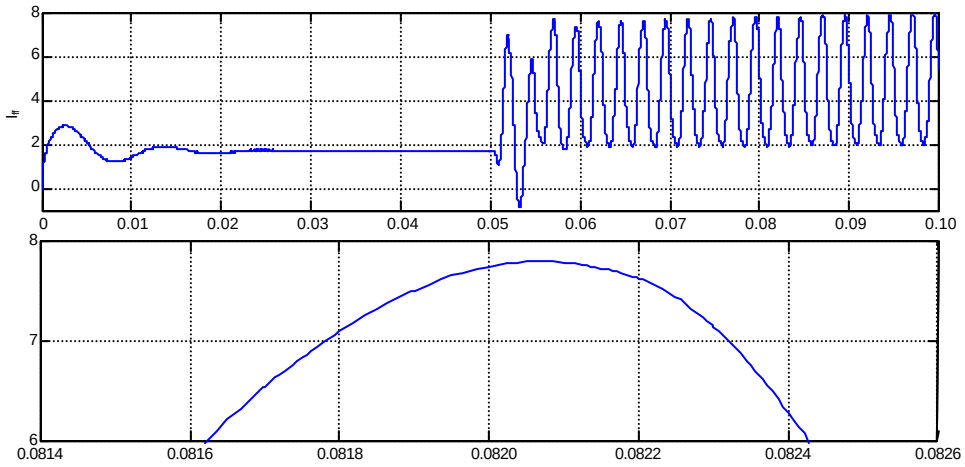

Fig. 10: Exciter stator current I_{ff} under one diode short-circuit fault

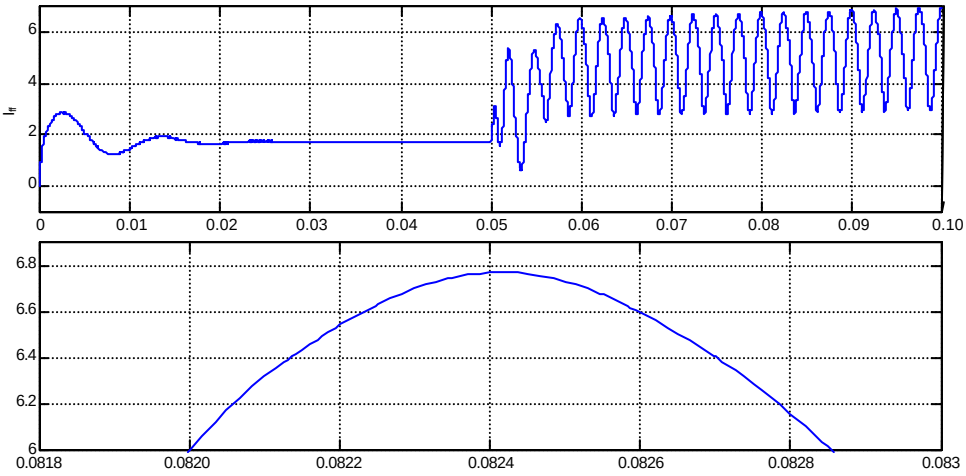

Fig. 11: Exciter stator current I_{ff} under two diodes short-circuit in the same bridge-arm fault

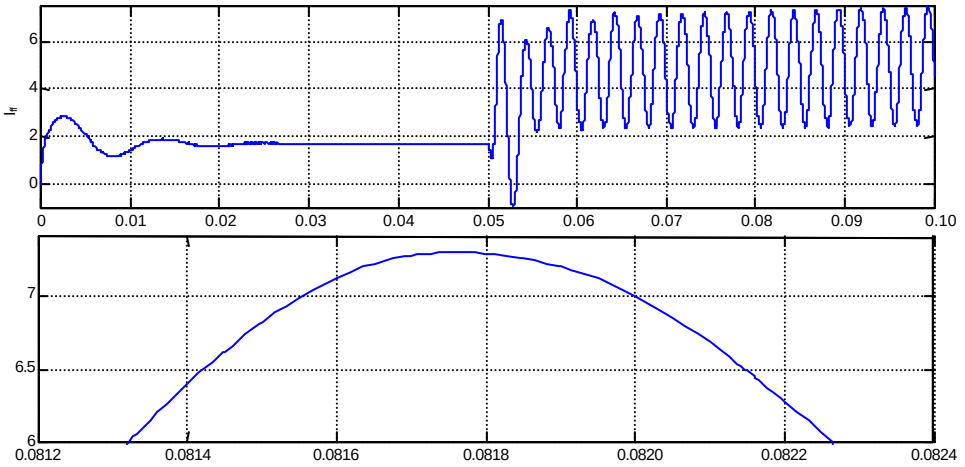

Fig. 12: Exciter stator current I_{ff} under two diodes short-circuit in different phases and bridge- arms fault

Table 2: Harmonic analysis of I_{ff} before and after rotating rectifier faults

	Feature vector						
Fault type	T1	T2	T3	T4	T5	T6	T7
Normal state	1.229×10^{-4}	6.234×10^{-5}	4.954×10^{-5}	5.197×10^{-5}	3.637×10^{-5}	7.614×10^{-3}	3.608>
One diode open-circuit	4.251×10^{-3}	4.375×10^{-3}	2.227×10^{-3}	4.000×10^{-5}	1.495×10^{-3}	5.831×10^{-3}	8.213>
Two diodes open-circuit in one-phase	1.695×10^{-4}	8.828×10^{-3}	9.172×10^{-5}	1.080×10^{-4}	4.122×10^{-5}	4.247×10^{-3}	2.880>
Two diodes open-circuit in the same bridge arm	6.040×10^{-3}	1.927×10^{-3}	2.365×10^{-3}	1.674×10^{-3}	4.394×10^{-4}	3.999×10^{-3}	5.219>
Two diodes open-circuit in different phase and bridge arm	5.957×10^{-3}	2.702×10^{-3}	1.785×10^{-3}	1.654×10^{-3}	1.136×10^{-3}	4.925×10^{-3}	7.798×10^{-3}
One diode short-circuit	0.676	1.043	4.158×10^{-2}	1.480×10^{-2}	3.023×10^{-3}	3.017×10^{-3}	1.274×10^{-3}
Two Diodes short-circuit in the same bridge arm	0.81	4.547×10^{-2}	1.686×10^{-2}	6.428×10^{-3}	2.392×10^{-3}	2.023×10^{-3}	1.035×10^{-3}
Two diodes short-circuit in different phases and bridge arms	0.510	1.796×10^{-2}	1.556×10^{-2}	1.108×10^{-2}	4.283×10^{-3}	3.745×10^{-3}	6.584×10^{-4}

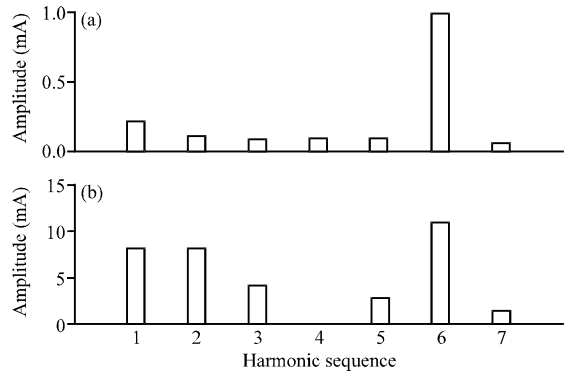

Fig. 13: Harmonic analysis of I_{ff} in normal state and one diode open-circuit fault

FAULT FEATURE EXTRACTION OF RORATING RECTIFIER

Signal feature extraction plays an important in fault diagnosis. To identify the type of the fault, the fault signal should firstly be quantified. Harmonic analysis based on Fourier Transform can be a good method of analyzing the properties of stationary signals (Boggess and Narcowich, 2002; Gray *et al*., 2009). The exciter stator field current I_{ff} in the three-level generator system is analyzed by the FFT algorithm. The amplitudes of each harmonic is extracted and form the feature vector T of the signal, laying the foundation for fault diagnosis.

As known from the simulation results in Fig. 5, I_{ff} is basically a stationary signal by the role of the AVR, ensuring the applicability of the Fourier analysis. Take the one diode open-circuit fault as an example, harmonic analysis of I_{ff} is proceeded before and after the fault and the result is shown in Fig. 13. Figure 13a and b are respectively the fundamental and 2nd-7th harmonic analysis histograms of I_{ff} in normal state and one diode open-circuit fault.

As seen from the figure, when the three-phase brushless exciter operates normally, the ripple wave in stator current I_{ff} is mainly the 6th harmonic. When one diode open-circuit fault occurs in rotating rectifier, I_{ff} also contains a large fundamental and 2nd harmonic except the 6th harmonic. The simulation results is consistent with the theoretical analysis.

And then harmonic analysis is carried out on I_{ff} obtained from simulation experiments of the other six faults. The results are normalized by the DC component and all harmonics constitute the feature vector T of signal, as shown in Table 2.

T_1 to T_7 are respectively the ratios between the fundamental to 7th harmonic and the DC component. These ratios constitute the feature vector T of I_{ff} and can be further applied for fault diagnosis and identification by algorithmic tools such as neural network.

CONCLUSION

When faults occur in rotating rectifier of aircraft IDG, the AC exciter armature current will change, causing the armature field changed and then effecting harmonic characteristics of excitation winding by the armature reaction. The faults are ultimately reflected through the exciter stator field current. The working condition of rotating rectifier can be well reflected by the harmonic characteristic of the stator current. The condition of each faulted bridge-arm of rotating rectifier can be obtained by harmonic analysis of the stator current. Then the feather vector of fault signal is extracted based on harmonic analysis, laying the foundation for the fault diagnosis and effectively improving the level of fault detection and diagnosis of rotating rectifier.

ACKNOWLEDGMENTS

This study is supported by the National Nature Science Foundation of China (51277011), the Tianjin Key Technology R and D Program (11ZCKFGX04000), the Fundamental Research Funds for the Central Universities (ZXH2012B002, ZXH2012C006 and 3122013P005), the Open Foundation of Ground Support Equipments Research Base of Civil Aviation University of China and the Innovation Experiment Technology Foundation of Civil Aviation University of China.

REFERENCES

Batzel, T.D., D.C. Swanson and J.F. Defenbaugh, 2003. Predictive diagnostics for the main field winding and rotating rectifier assembly in the brushless synchronous generator. Proceedings of the 4th IEEE International Symposium on Diagnostics for Electric Machines, Power Electronics and Drives, August 24-26, 2003, Atlanta, GA., USA., pp: 349-354.

Boggess, A. and F.J. Narcowich, 2002. A First Course in Wavelets with Fourier Analysis. Prentice Hall, Upper Saddle River, NJ..

Gray, D., Z. Zhang, C. Apostoaia and C. Xu, 2009. A neural network based approach for the detection of faults in the brushless excitation of a synchronous motor. Proceedings of the IEEE International Conference on Electro/Information Technology, June 7-9, 2009, Windsor, ON., USA., pp: 423-428.

Hydro-Qubec, 2008. SimPowerSystemsTM for User's Guide. The Math Works Inc., Natick, MA., USA.

Li, F. and D. Zhu, 2007. Electromechanics. Science Press, Beijing, China.

Mouni, E., S. Tnani and G. Champenois, 2008. Synchronous generator modelling and parameters estimation using least squares method. Simul. Modell. Pract. Theory, 16: 678-689.

Na, W., 2011. A feedforward controller for a brushless excitation system during the diode open circuit fault operation. Proceedings of the IEEE Power and Energy Society General Meeting, July 24-29, 2011, San Diego, CA., USA., pp: 1-4.

Wakileh, G.J., 2011. Power Systems Harmonics: Fundamentals, Analysis and Filter Design. China Machine Press, Beijing, China.

Wang, T., N. Liu, C. Xie and K. Sun, 2006. Study of fault diagnosis in brushless machines based on artificial immune algorithm. Proceedings of the IEEE International Symposium on Diagnostics for Electric Machine, Industrial Electronics, July 9-13, 2006, Montreal, Canada, pp: 1779-1782.

Zhang, C. and L. Xia, 2009. Fault diagnosis of generator rotating rectifier based on fractal and dynamics. Electr. Mach. Control, 13: 6-10.